

Evidence for monopoles in the quantized $SU(2)$ lattice vacuum: a study at finite temperature

M.L. Laursen¹ and G. Schierholz²

¹ NORDITA DK-2100 Copenhagen, Denmark

² Institut für Theoretische Physik der Universität, D-2300 Kiel, and Deutsches Elektronen-Synchrotron DESY, D-2000 Hamburg 52, Federal Republic of Germany

Received 9 October 1987

Abstract. In $SU(2)$ gauge theory colour confinement occurs if the vacuum condenses into a coherent monopole plasma. To verify this picture, the first question to be answered is whether the vacuum supports monopoles at all. Since we expect the monopoles to be dilute and massive in the deconfinement phase, we begin the search there. The method relies on cooling equilibrium lattice gauge field configurations—which are generated at the appropriate temperature—until the underlying semi-classical solutions emerge. We then pass to the confinement region and ask whether the monopoles condense. Finally, we repeat the procedure for gauge group $SU(3)$. The results confirm our expectations.

I Introduction

The present paper continues previous efforts [1] to reach an intuitive understanding of the QCD vacuum and the dynamics that drives it using the lattice formulation and numerical simulations.

A first step in this direction is to look for the underlying semi-classical structure. So far, we have learned [1, 2] that the vacuum of the pure $SU(2)$ gauge theory at zero temperature carries instantons. This result is maybe not surprising, but we consider it the first proof that semi-classical ideas are indeed relevant for parameterizing the vacuum state.

While instantons offer an intuitive understanding of topology (as described by the Pontryagin index) and its implication for QCD, they (alone) cannot give confinement. 't Hooft [3] and Mandelstam [4] have argued that the confinement phase is a coherent plasma of colour-magnetic monopoles, just as the superconducting phase is a coherent plasma of charges. In this picture colour-electric flux cannot spread out unless it is squeezed into tubes of quantized flux, which

ensures quark confinement. Similar ideas have also been formulated by Mack [5].

In pure Yang-Mills theories colour-magnetic monopoles (can) arise in the presence of dynamically generated Higgs fields as time-independent (particle-like) solutions of finite energy to the classical field equations. In the confinement phase the monopoles must become very light, formally even

$$M^2 < 0 \tag{1}$$

(M : monopole mass), in order to induce a colour-magnetic Higgs mechanism, which is the condition for colour-magnetic superconductivity. In the deconfinement phase, on the other hand, we may expect the monopoles to be massive and dilute.

This picture can be tested by cooling [1] equilibrium lattice gauge field configurations. If it is correct, we should find monopoles accompanied by a plateau in the action in the deconfinement phase, whereas in the confinement phase the action should decay rapidly to zero, modulo instanton configurations, due to the effectively vanishing monopole mass.

The purpose of the present paper is to carry out this test. The paper is organized as follows. In Sect. II we briefly review the characteristic features of $SU(2)$ monopoles. Section III presents evidence that the $SU(2)$ lattice vacuum carries colour-magnetic monopoles in the deconfinement phase. In Sect. IV we ask whether the monopoles condense to a coherent plasma when we pass to the confinement phase. Section V repeats the search for monopoles for gauge group $SU(3)$. Finally, in Sect. VI we draw the conclusion.

II A profile of $SU(2)$ monopoles

Consider a $SU(2)$ Yang-Mills field coupled to an adjoint Higgs field in the continuum. The Lagrangian

density for the model is

$$\mathcal{L} = \text{Tr} \left\{ -\frac{1}{2g^2} F_{\mu\nu} F_{\mu\nu} - D_\mu \phi^\dagger D_\mu \phi - \lambda(\phi^\dagger \phi - \frac{1}{2}v^2)^2 \right\}, \quad (2)$$

where

$$D_\mu \phi = \partial_\mu \phi + [A_\mu, \phi], \quad A_\mu = \frac{\sigma^a}{2i} A_\mu^a, \quad \phi = \frac{\sigma^a}{2i} \phi^a. \quad (3)$$

We are looking for finite energy solutions. The energy of a field configuration is

$$E = \int d^3x \left\{ \frac{1}{2g^2} [E_i^a E_i^a + B_i^a B_i^a] + \frac{1}{2} (D_i \phi)^a (D_i \phi)^a + \frac{\lambda}{8} (\phi^a \phi^a - v^2)^2 \right\}, \quad (4)$$

Finiteness of (4) requires that

$$|\phi| = \text{Tr}(\phi^\dagger \phi)^{1/2} = (\phi^a \phi^a)^{1/2} \xrightarrow{|\mathbf{x}| \rightarrow \infty} v, \quad (5)$$

$$(D_i \phi)^a \xrightarrow{|\mathbf{x}| \rightarrow \infty} 0. \quad (6)$$

Equation (5) implies that $|\phi| = v$ at each point on the 2-sphere at spatial infinity, S_∞^2 , but it places no restriction on the orientation of ϕ . The space of possible orientations is isomorphic to the 2-sphere S^2 . Thus, associated with every finite-energy field configuration is a mapping

$$\hat{\phi}: S_\infty^2 \rightarrow S^2, \quad \hat{\phi} = |\phi|^{-1} \phi. \quad (7)$$

This mapping has a winding number q . Because it is an integer, it is preserved by smooth deformations of the fields within a finite energy sector. Hence, it is a topological invariant.

Define now the conserved magnetic current [6]

$$j_\mu = \epsilon_{\mu\nu\rho\sigma} \partial_\nu f_{\rho\sigma}, \quad (8)$$

where $f_{\mu\nu}$ is 't Hooft's Abelian electromagnetic field tensor [7] which refers to fields in the gauge $\sigma^3/2i = V \hat{\phi} V^{-1}$ [8], i.e. where $\hat{\phi}$ is diagonal,

$$f_{\mu\nu} = \partial_\mu a_\nu - \partial_\nu a_\mu, \quad a_\mu = -i \text{Tr} \{ \sigma^3 V (A_\mu + \partial_\mu) V^{-1} \}. \quad (9)$$

Then one can write

$$q = \frac{1}{8\pi} \int d^3x j_0 = \frac{1}{4\pi} \int_{S_\infty^2} d^2x_i b_i, \quad b_i = \frac{1}{2} \epsilon_{ijk} f_{jk} \quad (10a)$$

$$= \frac{1}{4\pi} \int_{S_\infty^2} d^2x_i \epsilon_{ijk} \text{Tr} \{ \hat{\phi} [\partial_j \hat{\phi}, \partial_k \hat{\phi}] \}. \quad (10b)$$

It is readily checked that the rhs of (10b) equals the number of times the vector $\hat{\phi}$ covers the unit sphere $|\hat{\phi}| = 1$. The rhs of (10a) is the magnetic flux through S_∞^2 . Hence, q counts the magnetic charge in 3-space. Since j_μ vanishes everywhere except at the zeros of the

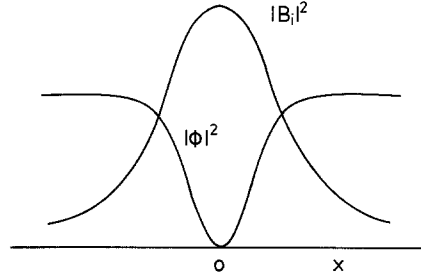


Fig. 1. Sketch of Higgs field $|\phi|^2$ and colour magnetic field $|B_i|^2$ in a monopole field configuration

Higgs field ϕ , x_0 , (10) can be written

$$q = \frac{1}{4\pi} \sum_{x_0} \int_{S_\varepsilon^2} d^2x_i b_i = \frac{1}{4\pi} \sum_{x_0} \int_{S_\varepsilon^2} d^2x_i \epsilon_{ijk} \text{Tr} \{ \hat{\phi} [\partial_j \hat{\phi}, \partial_k \hat{\phi}] \}, \quad (11)$$

where $S_\varepsilon^2(x_0)$ is the infinitesimal sphere surrounding x_0 .

Equation (6) implies that the gauge field at spatial infinity must be a pure gauge. A classical field configuration with unit magnetic charge, a monopole, will therefore be of the form shown in Fig. 1. It consists of a central region, in which the magnetic field is concentrated and the Higgs field ϕ has a zero, and an outside region with asymptotically vanishing magnetic field and constant Higgs field. The simplest such field configuration, where $\hat{\phi}$ is the identity map, is the famous 't Hooft-Polyakov monopole [7, 9].

A non-vanishing magnetic charge q is followed by zero modes in the spectrum of the 3-dimensional Dirac operator [10]

$$\gamma_i (\partial_i + iA_i) + \mu \phi. \quad (12)$$

The index theorem due to Callias [11] states that

$$q = n_+ - n_-, \quad (13)$$

where n_+ (n_-) is the number of right-handed (left-handed) zero modes. The operator (12) describes the motion of a fermion in the background of a static field configuration. The index is independent of μ .

In the pure Yang-Mills theory there is no elementary Higgs field. At finite temperature we may take the time component of the gauge field, A_0 , in the gauge $\partial_0 A_0 = 0$ as dynamically generated adjoint Higgs field. This is feasible because A_0 cannot be gauge transformed to zero.

On the lattice the Abelian field tensor $f_{\mu\nu}$ is related to the Abelian parallel transport around a plaquette,

$$u_{x,\mu\nu} = u_{x,\mu} u_{x+\hat{\mu},\nu} u_{x+\hat{\mu},\mu}^* u_{x,\nu}^*, \quad u_{x,\mu} = \exp \{ i \arg (V_x U_{x,\mu} V_{x+\hat{\mu}}^{-1}) \}, \quad (14)$$

where $U_{x,\mu}$ is the usual $SU(2)$ link matrix, so that the

magnetic charge inside a spatial cube $c(x)$ is [8]

$$q(c(x)) = \frac{1}{4\pi} \sum_{u_{x,ij} \in \partial c(x)} \arg u_{x,ij}. \quad (15)$$

The phases are restricted to $|\arg u_{x,ij}| \leq \pi$, and $u_{x,ij}$ has the orientation of $\partial c(x)$. The sum of $q(c(x))$ over all cubes is zero.

The index theorem (13) holds naturally only on open spaces. But we believe that a well separated monopole-antimonopole pair on the lattice will give rise to two zero modes and, what we will encounter in this paper, that a monopole and a “spurious” antimonopole will give rise to one zero mode.

III Search for monopoles at finite temperature

Our first question is: does the $SU(2)$ vacuum in the finite temperature deconfinement phase have an underlying monopole structure? To answer this question we proceed in two steps. First, we generate equilibrium lattice gauge field configurations at the desired temperature. Then, we cool these configurations by a suitable relaxation method such that after a number of sweeps through the lattice we are left with the underlying solutions to the classical field equations.

We use Wilson’s action

$$S = \beta \sum_{\substack{x \\ \mu < \nu}} (1 - \frac{1}{2} \text{Tr} U_{x,\mu\nu}) \\ = \beta \sum_{\substack{x \\ \mu < \nu}} [1 - \frac{1}{2} \text{Tr} (U_{x,\mu} U_{x+\hat{\mu},\nu} U_{x+\hat{\mu},\mu}^+ U_{x,\nu}^+)] \quad (16)$$

with periodic boundary conditions for equilibration. To relax the quantum fluctuations we replace each link matrix $U_{x,\mu}$ successively by

$$c \sum_{\nu \neq \mu} [U_{x,\nu} U_{x+\hat{\nu},\mu}^+ U_{x+\hat{\nu},\nu} + U_{x-\hat{\nu},\nu}^+ U_{x-\hat{\nu},\mu} U_{x+\hat{\nu}-\hat{\nu},\nu}], \quad (17)$$

where c is a normalization factor such that (17) is a

Table 1. The sample of $SU(2)$ gauge field configurations investigated in the course of this work

β	Lattice size	# Configurations
2.4	$8^3 \cdot 4$	100
	$10^3 \cdot 4$	100
	$14^3 \cdot 4$	20
2.2		40
2.25		40
2.3		40
2.325	$8^3 \cdot 4$	50
		55
		60
2.45	$12^3 \cdot 6$	60
2.5		60
2.56		60
2.3	$10^3 \cdot 2$	20
	$10^3 \cdot 3$	20

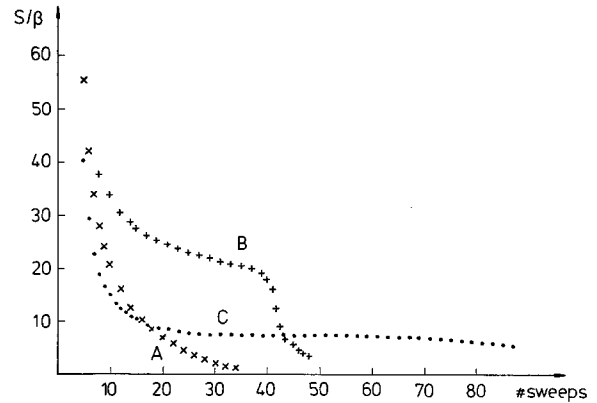


Fig. 2. S/β as a function of the number of cooling sweeps for 3 typical $SU(2)$ gauge field configurations

$SU(2)$ matrix. This means that each link matrix is replaced by the sum of all parallel transporters which form a plaquette with $U_{x,\mu}^+$. When all link matrices have been replaced we call this one sweep. Experience has shown [1] that after a number of sweeps the action either goes to zero, in which case the field configuration has decayed into the trivial vacuum, or it ends up in a plateau. On the plateau

$$\frac{\delta S}{\delta U_{x,\mu}} = 0, \quad (18)$$

which is the lattice analogue of the classical field equations.

In the course of this work we have investigated a large sample of lattice gauge field configurations, each of which contains at least about a thousand sweeps for equilibration, and individual gauge field configurations in the sample are separated by a further 50 sweeps. The sample is listed in Table 1.

We begin our search by cooling gauge field configurations on $10^3 \cdot 4$ lattices, which were equilibrated at $\beta = 2.4$. This corresponds to a temperature that lies well above the deconfinement phase transition temperature [12]. In Fig. 2 we show the history of 3 typical such field configurations as a function of the number of cooling sweeps. Configuration A decays into the trivial vacuum. Configuration B shows a plateau at

$$S \approx \beta 2\pi^2, \quad (19)$$

which suggests that it carries an (anti)instanton. Upon a closer look—i.e. by computing the energy density, the topological charge and the eigenvalues of the fermion matrix for staggered fermions [1]—this proves indeed to be the case. Instanton configurations are, however, rare. More often we find configurations of type C, which show a plateau of about half the height of an (anti)instanton configuration. On the plateau the topological charge is zero, and we also observe no approximate zero mode in the eigenvalue spectrum of the fermion matrix. This indicates that the solutions to the classical field equations we have

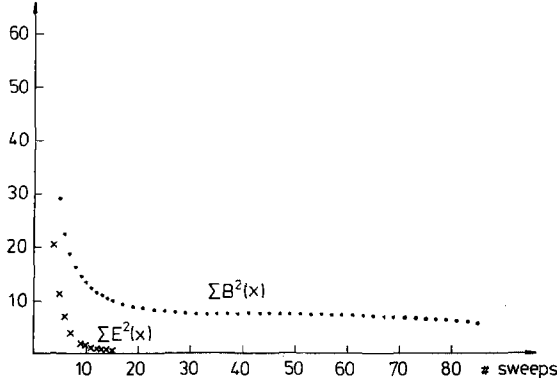


Fig. 3. The colour electric and magnetic field strengths shown separately for configuration C

found are something new. In the following we shall show that they are (anti)monopoles.

To qualify as monopoles, the field configurations must be static modulo gauge transformations, their energy density must be localized in space, they must have a magnetic charge and give rise to zero modes in the spectrum of the 3-dimensional Dirac operator.

(a) Static solution

Defining the colour electric and magnetic fields

$$E^2(x) = \sum_i (1 - \frac{1}{2} \text{Tr} U_{x,0i}) \quad (20)$$

and

$$B^2(x) = \sum_{i<j} (1 - \frac{1}{2} \text{Tr} U_{x,ij}), \quad (21)$$

respectively, we can write

$$\beta^{-1} S = \sum_x (E^2(x) + B^2(x)). \quad (22)$$

In Fig. 3 we have shown both contributions separately for configuration C. On the plateau we find

$$E^2(x) \simeq 0. \quad (23)$$

This is a sufficient condition for the configuration to be static. Equation (23) indicates furthermore that the configuration is not self-dual.

(b) Energy

To see whether the energy is localized in space, we have computed the energy density

$$D(x) = \frac{1}{3} \sum_{i<j} (1 - \frac{1}{2} \text{Tr} U_{x,ij}) = \frac{1}{3} B^2(x). \quad (24)$$

On the plateaus we find that the energy is concentrated in "lumps". In Fig. 4 we show the energy density for a 2-dimensional cross section through the center of such a "lump". The units are $[10 D(x)]$. It is striking that the energy density falls off much slower than the action density does in case of an instanton [1]. This is what we expect for an (anti)monopole configuration.

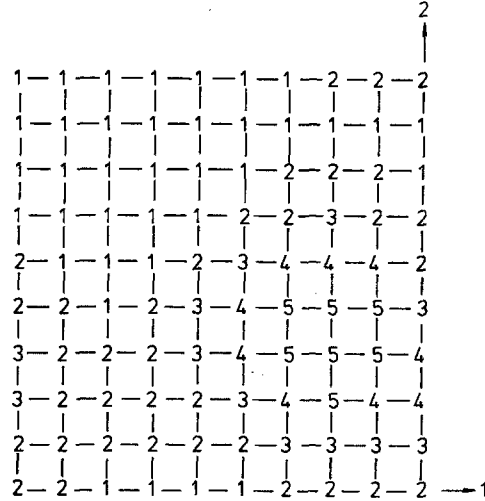


Fig. 4. The action density $[10 D(x)]$ for a 2-dimensional cross section through the center of the "monopole"

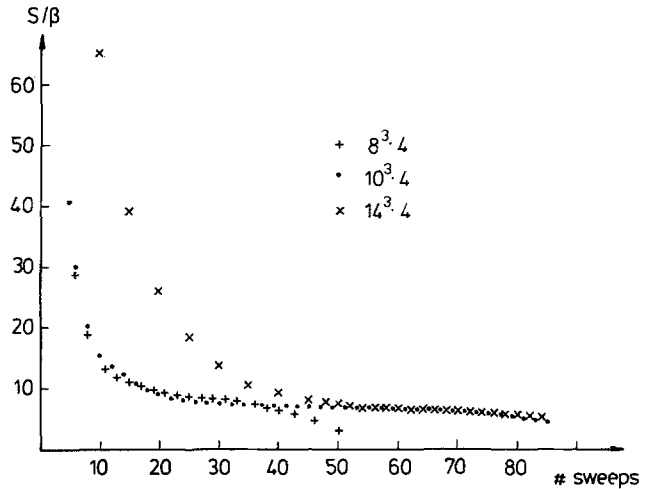


Fig. 5. Comparison of the "monopole" action on $8^3 \cdot 4$, $10^3 \cdot 4$ and $14^3 \cdot 4$ lattices

The total energy seems also to be roughly independent of the spatial size of the lattice as it should be for a genuine monopole: in Fig. 5 we compare $\beta^{-1} S$ for 3 typical configurations on $8^3 \cdot 4$, $10^3 \cdot 4$ and $14^3 \cdot 4$ lattices, respectively, which were equilibrated at $\beta = 2.4$. The height of the plateau is about the same. Later on we shall argue that the energy scale is given by the temperature.

(c) Magnetic charge

A necessary condition for the configuration in Fig. 4 to carry a magnetic charge is that the Higgs field, in our case A_0 , has a zero. We have transformed the gauge field configuration to the gauge $\partial_0 A_0 = 0$ and computed A_0 from the Polyakov loop

$$L(x) = \text{Tr} \prod_{n=0}^{L_t-1} U_{x+n\hat{0},0} = \text{Tr} e^{[dt A_0]} = \text{Tr} e^{\tau^{-1} A_0}, \quad (25)$$

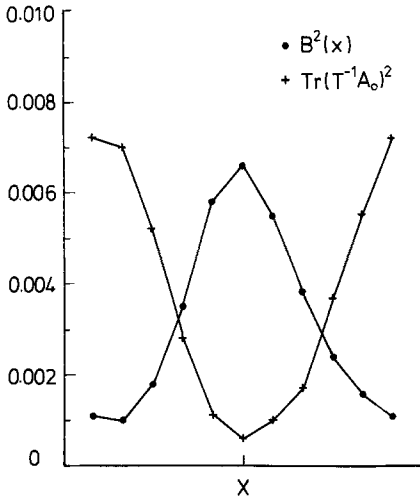


Fig. 6. $B^2(x)$ and $\text{Tr}(T^{-1}A_0)^2$ for a 1-dimensional cross section through the center of the “monopole” of Fig. 4

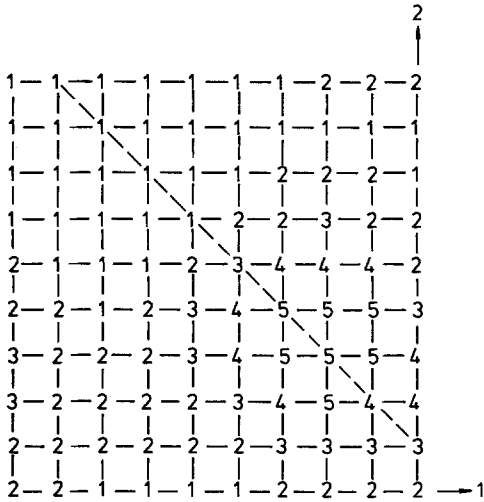


Fig. 7. The 1-dimensional section through the center of the “monopole”

where L_t is the number of time slices and T denotes the temperature. The result is shown in Fig. 6, where we have plotted $\text{Tr}(T^{-1}A_0)^2$ and $B^2(x)$ for a 1-dimensional cross section through the center of the “lump”. The section is indicated by the dashed line in Fig. 7. We see that A_0 is indeed approximately zero at the peak of $B^2(x)$. We also find close resemblance to the monopole configuration sketched in Fig. 1.

Now we turn to the quantitative analysis. Using the algorithm developed in [8], we have computed $q(c(x))$ for all spatial cubes $c(x)$ for the configuration in Fig. 4. Since the field configuration is static, we can restrict ourselves to a single time slice. We find that $q(c(x))$ is zero except for two cubes, for which $q = +1$ and $q = -1$, respectively. The position of these cubes is marked by circles in Fig. 8. The plane at the bottom is the plane shown in Fig. 4, and the area encircled is the central region ($[10 D(x)] \geq 5$). This indicates that

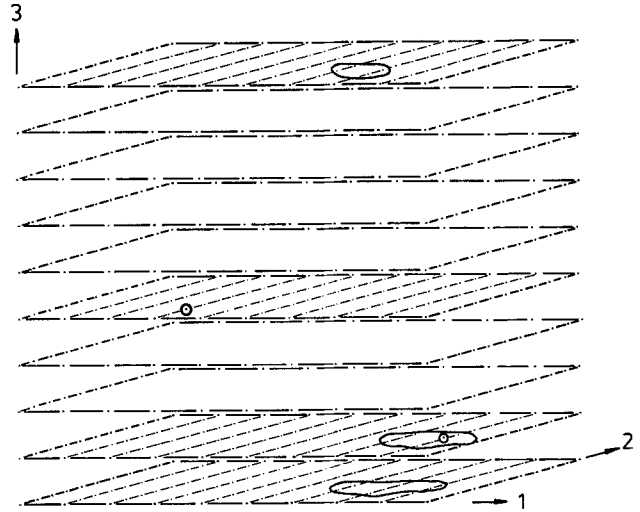


Fig. 8. A time slice of the “monopole” configuration of Fig. 4. The encircled area indicates the central region of the “monopole”. The circles mark the position of cubes which carry one unit of magnetic charge each

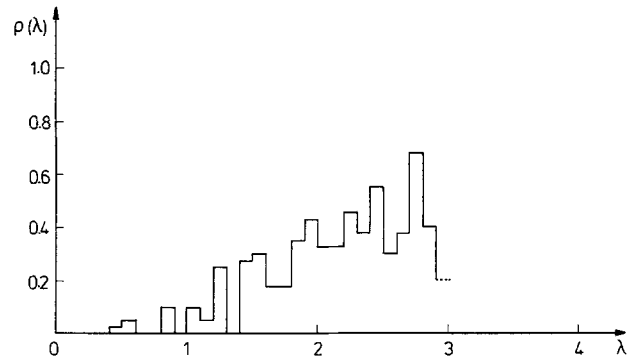


Fig. 9. The eigenvalue density of the 3-dimensional Dirac operator in the background of configuration A after 30 cooling sweeps

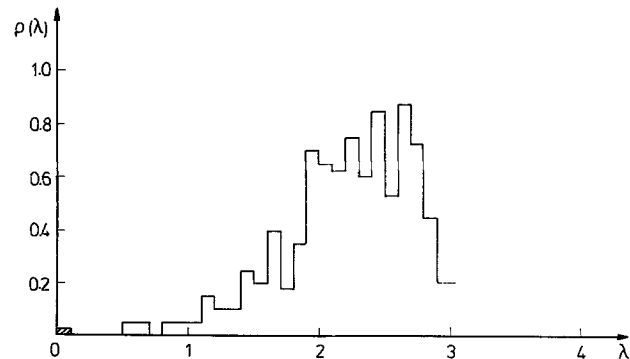


Fig. 10. The eigenvalue density of the 3-dimensional Dirac operator in the background of the “monopole” configuration C after 30 cooling sweeps

the “lump” carries one unit of magnetic charge in the central region. The other cube lies in the region where $B^2(x) \approx 0$. It is associated with a second zero of the Higgs field A_0 , which has to appear somewhere as a consequence of the periodic boundary conditions. Note that this “spurious” charge costs practically no energy.

(d) Zero modes

We shall now investigate the eigenvalue spectrum of the latticized 3-dimensional Dirac operator (12) in the limit $\mu \rightarrow 0$. We choose staggered fermions for obvious reasons. The corresponding matrix connecting the lattice sites is

$$M_{x,x+\hat{i}} = (-1)^{\delta_1 + \dots + \delta_{i-1}} U_{x,i} \quad M_{x+\hat{i},x} = -M_{x,x+\hat{i}}^+ \tag{26}$$

The boundary conditions are taken to be antiperiodic. To compute the eigenvalues of (26) we use the Lanczos algorithm [13].

We start by computing the eigenvalue spectrum in the background of configuration A (cf. Fig. 1) after 30 cooling sweeps, where it has decayed into the trivial vacuum. We expect no small eigenvalues. The result is shown in Fig. 9, which confirms that. Next we compute the eigenvalue spectrum in the background of configuration C after 30 cooling sweeps. The result is shown in Fig. 10. In accord with the index theorem (13) we find “one” approximate zero mode, which in fact is twofold degenerate due to the flavour degeneracy of the staggered fermions. The result is typical of many other configurations.

This finishes the “proof” that the new objects we have found are indeed (anti)monopoles.

Before we continue with the next subject we like to report one more result on zero modes. A 3-dimensional section of an instanton through its center is a dyon [14], which carries one unit of magnetic charge. We therefore expect the 3-dimensional Dirac operator to have one zero mode on this section and none else. In Table 2 we list the lowest eigenvalue of the instanton configuration B (cf. Fig. 1) after 30 cooling sweeps for each time slice. The instanton sits on the fourth time slice. This confirms our expectation.

(e) Stability

We have studied in detail [1] what causes the instanton configurations to decay to the trivial vacuum: as we

Table 2. Smallest eigenvalues of the 3-dimensional Dirac operator in the background of a 3-dimensional section of an instanton at fixed times

Time slice	Smallest eigenvalue
1	0.449
2	0.614
3	0.395
4	0.065

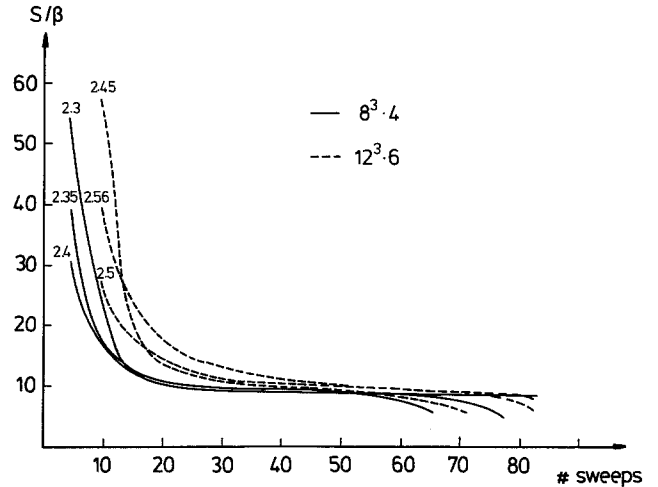


Fig. 11. Comparison of the “monopole” action at varying temperatures: $\beta = 2.3, 2.35, 2.4$ on $8^3 \cdot 4$ lattices and $\beta = 2.4, 2.5, 2.56$ on $12^3 \cdot 6$ lattices

approach the end of the plateau, the instantons shrink, become a dislocation [15] and finally are annihilated. The situation is different for the monopole configurations. At the end of the plateau we observe that the cubes, which carry the magnetic charge of the “genuine” (say) monopole and the “spurious” anti-monopole (cf. Fig. 8), respectively, move towards each other until they coincide and all local charges are zero. This means that the “genuine” monopole and the “spurious” antimonopole annihilate each other. The annihilation process starts rather abruptly and takes only a few cooling sweeps to complete.

We have checked that the monopole configurations are to some extent stable against quantum fluctuations. This was done by heating the configurations with about 30 Monte Carlo sweeps and then cooling them again. We got the monopole configurations back. They moved, however, in 3-space.

(f) Monopole mass

Monopoles are solutions of finite energy and hence carry a scale, the monopole mass. A priori there is no reason why the mass should be quantized. But this seems to be the case: above we have seen that the action of the monopole configurations on $L_t = 4$ lattices at $\beta = 2.4$ clustered around half the instanton action. We shall investigate this circumstance in more detail now.

To do so we cool configurations on lattices of various temporal extents and couplings—and hence of varying temperatures $T = 1/L_t a$ (a : lattice spacing). The results are shown in Fig. 11 for a few representative configurations. They are on $8^3 \cdot 4$ lattices at $\beta = 2.3, 2.35$ and 2.4 and on $12^3 \cdot 6$ lattices at $\beta = 2.45, 2.5$ and 2.56 . We find that the height of the plateaus is roughly the same in all cases:

$$\beta^{-1} S = E/T = M/T \approx \text{const.} \tag{27}$$

($E(M)$: monopole energy (mass)). This requires

$$M \sim T. \quad (28)$$

If we take only those plateaus into account where $\beta^{-1}S$ changes by less than 1 over at least 20 cooling sweeps, we obtain furthermore

$$\beta^{-1}S = 9 - 10 \quad (29)$$

and the monopole mass

$$M = (9 - 10)T. \quad (30)$$

This result is not really surprising. It reflects that the physics of the spatial degrees of freedom at finite temperature is determined by the dynamics of the corresponding 3-dimensional theory at zero temperature with coupling g^2T [16].

IV The transition region

What happens now to the monopoles when we pass to the confinement region? Do they condense? To try to answer this question we have computed the “density” of monopoles as a function of the temperature. The result is compiled in Figs. 12 and 13 for two lattice sizes: $8^3 \cdot 4$ and $12^3 \cdot 6$. In Fig. 12 we show the frequency ν_M of finding an (anti)monopole configuration (basically a plateau). Each entry is based on 40–60 equilibrium gauge field configurations. In Fig. 13 we show the density

$$\rho_M = \nu_M / (L_s a)^3, \quad (31)$$

where L_s is the spatial extent of the lattice. For the lattice spacing we have assumed the 2-loop formula

$$a = \Lambda_L^{-1} \left(\frac{6\pi^2}{11} \beta \right)^{51/121} e^{-(3\pi^2/11)\beta}. \quad (32)$$

The units are Λ_L^3 . The shaded area indicates the location of the deconfinement phase transition. Note that the values at the lowest temperature have errors. This is due to the fact that the plateaus become by and large shorter and sometimes are not unambiguously identifiable as monopole configurations. We find that the monopole “density” decreases rapidly as we enter the confinement region. The “density” reported here should not be confused with the genuine monopole density computed in [8]. Rather, it should be noted that a very light monopole or a coherent plasma of them will not show a plateau and hence will not be counted.

We shall compare this result now with the equivalent quantities for instantons. Based upon the same sample of gauge field configurations we have computed the frequency ν_I of finding an (anti)instanton and the instanton “density”

$$\rho_I = \nu_I / L_s^3 L_t a^4. \quad (33)$$

The quantities ν_I and ρ_I are shown in Figs. 12 and 13, respectively. In this case we find the opposite

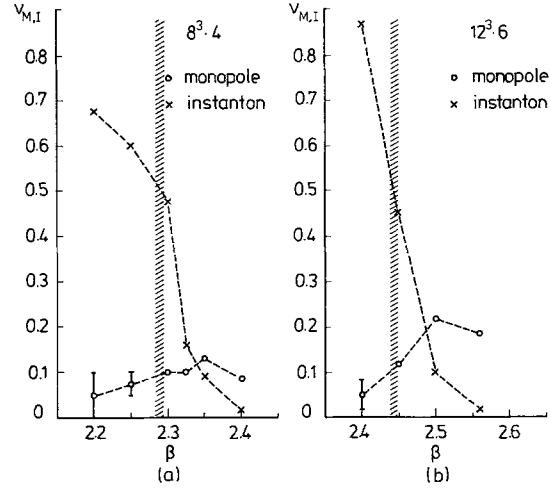


Fig. 12a, b. The frequency $\nu_{M(I)}$ of monopole (instanton) configurations on a $8^3 \cdot 4$ and b $12^3 \cdot 6$ lattices. The shaded area marks the location of the deconfinement phase transition

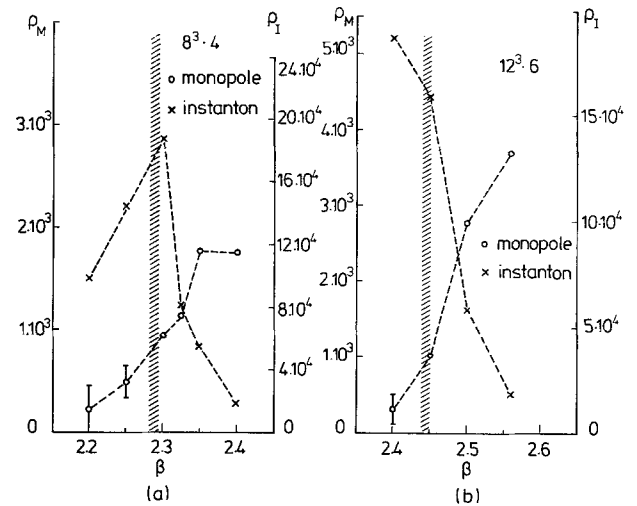


Fig. 13a, b. The “density” $\rho_{M(I)}$ of monopole (instanton) configurations on a $8^3 \cdot 4$ and b $12^3 \cdot 6$ lattices

picture: the instanton “density” drops sharply as we enter the deconfinement region.

In [8] it was found that the genuine monopole density is large in the confinement phase and small in the deconfinement phase. For an update see also [17]. Not answered was the question whether the monopoles condense. The present work indicates that this is the case, because the only explanation we can think of which is consistent with both results is that the monopoles become very light and coherent as we enter the confinement region.

V $SU(3)$

We shall extend the search for monopoles now to the gauge group $SU(3)$. We use Wilson’s action

$$S = \beta \sum_{\substack{x \\ \mu < \nu}} (1 - \frac{1}{3} \text{Re Tr } U_{x,\mu\nu}) \quad (34)$$

with periodic boundary conditions for equilibration. To relax the quantum fluctuations we follow Cabibbo and Marinari [8] and write the new link matrix

$$\begin{aligned} U_{x,\mu}^{(3)} &= \begin{pmatrix} \alpha^3 & 0 \\ 0 & 1 \end{pmatrix} U_{x,\mu}^{(2)} = \begin{pmatrix} \alpha^3 & 0 \\ 0 & 1 \end{pmatrix} \begin{pmatrix} 1 & 0 \\ 0 & \alpha^2 \end{pmatrix} U_{x,\mu}^{(1)} \\ &= \begin{pmatrix} \alpha^3 & 0 \\ 0 & 1 \end{pmatrix} \begin{pmatrix} 1 & 0 \\ 0 & \alpha^2 \end{pmatrix} \begin{pmatrix} \alpha_{11}^1 & 0 & \alpha_{12}^1 \\ 0 & 1 & 0 \\ \alpha_{21}^1 & 0 & \alpha_{22}^1 \end{pmatrix} U_{x,\mu}, \end{aligned} \quad (35)$$

where $\alpha^1, \alpha^2, \alpha^3$ are $SU(2)$ matrices and $U_{x,\mu}$ is the old $SU(3)$ link matrix. We compute α^1 first. Let us write

$$\begin{aligned} P &= \text{Re } U_{x,\mu} \sum_{\substack{v \neq \mu \\ v \neq \mu}} (U_{x,v} U_{x+\hat{v},\mu} U_{x+\hat{\mu},v}^+ \\ &\quad + U_{x-\hat{v},v}^+ U_{x-\hat{v},\mu} U_{x+\hat{\mu}-\hat{v},v}). \end{aligned} \quad (36)$$

We then choose

$$\alpha^1 = c \begin{pmatrix} P_{11}^* + P_{33} & -P_{13} + P_{31}^* \\ -P_{31} + P_{13}^* & P_{33}^* + P_{11} \end{pmatrix} \quad (37)$$

where c is a normalization factor such that the rhs is a $SU(2)$ matrix. Next we compute α^2 . For that we replace $U_{x,\mu}$ in equ. (36) by $U_{x,\mu}^{(1)}$ and call the result $P^{(1)}$. We then choose

$$\alpha^2 = c \begin{pmatrix} P_{22}^{(1)*} + P_{33}^{(1)} & -P_{23}^{(1)} + P_{32}^{(1)*} \\ -P_{32}^{(1)} + P_{23}^{(1)*} & P_{33}^{(1)*} + P_{22}^{(1)} \end{pmatrix}. \quad (38)$$

Finally we compute

$$\alpha^3 = c \begin{pmatrix} P_{11}^{(2)*} + P_{22}^{(2)} & -P_{12}^{(2)} + P_{21}^{(2)*} \\ -P_{21}^{(2)} + P_{12}^{(2)*} & P_{22}^{(2)*} + P_{11}^{(2)} \end{pmatrix}, \quad (39)$$

where $P^{(2)}$ is given by (36) with $U_{x,\mu}$ replaced by $U_{x,\mu}^{(2)}$. The choices (37), (38) and (39) minimize the action (34). When all link matrices $U_{x,\mu}$ have been exchanged by $U_{x,\mu}^{(3)}$ we call this one cooling sweep. In order to avoid getting trapped in metastable states we found it necessary to update the three $SU(2)$ submatrices in random order.

We have investigated 8^4 and $8^3 \cdot 4$ lattices at $\beta = 5.7$. The 8^4 lattices are in the confinement phase, whereas the $8^3 \cdot 4$ lattices are in the deconfinement phase. Both sets of lattices have been equilibrated by about a thousand sweeps. In Fig. 14 we show 3 typical 8^4 lattice configurations as a function of the number of cooling sweeps. Configurations A, B and C show plateaus at $\beta^{-1}S \approx 13, 26$ and 39 , respectively. This is what we expect for a 1-, 2-, and 3-(anti)instanton configuration:

$$\beta^{-1}S = \frac{4}{3}\pi^2 N, \quad N = 1, 2, 3. \quad (40)$$

We have not gone through all the tests to prove that they are indeed (anti)instantons. But we have checked that the action is localized. Now we turn to the $8^3 \cdot 4$ lattices in the deconfinement phase. In Fig. 15 we show a typical configuration. It shows a plateau at about

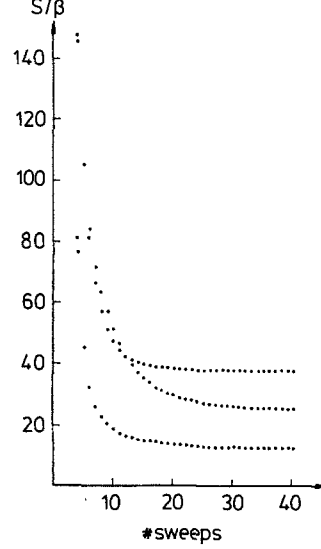


Fig. 14. S/β as a function of the number of cooling sweeps for 3 typical $SU(3)$ gauge field configuration in the confinement phase

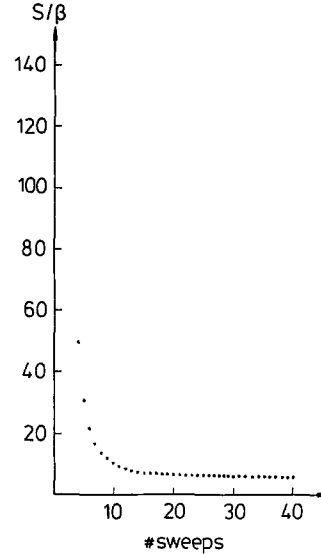


Fig. 15. S/β as a function of the number of cooling sweeps for a typical monopole configuration in the deconfinement phase

half the instanton action, i.e. $\beta^{-1}S \approx 6$. This configuration is a monopole configuration. Thus, we obtain the same picture as before also in $SU(3)$.

VI Conclusions

This work provides first evidence that $SU(2)$ and $SU(3)$ gauge theories support indeed an underlying monopole structure. The next step is to turn this picture into quantitative calculations. First promising results are already available [8, 17].

The conclusions so far are that the deconfinement phase is a dilute gas of monopoles, whereas evidence is mounting that the confinement phase can be understood as a coherent monopole plasma.

Acknowledgement. We would like to thank Meinulf Göckeler, Andreas Kronfeld and Uwe-Jens Wiese for most helpful discussions. One of us (G.S.) also likes to thank the participants of the Symposium on Topological and Geometrical Methods in Field Theory in Espoo, where the results of this paper were first reported [19], for their questions and comments.

References

1. E.-M. Ilgenfritz et al.: Nucl. Phys. B268 (1986) 693
2. J. Hoek: Comp. Phys. Commun. 39 (1986) 21; M. Teper: Phys. Lett. 162B (1985) 357
3. G. 't Hooft: In: High energy physics. Proceedings of the EPS International Conference, Palermo 1975, A. Zichichi (ed.). Bologna: Editrice Compositori 1976
4. S. Mandelstam: Phys. Rep. 23C (1976) 245
5. G. Mack: In: Recent developments in gauge theories. G. 't Hooft et al. (eds.) New York: Plenum 1980
6. J. Arafune, P.G.O. Freund, C.J. Goebel: J. Math. Phys. 16 (1975) 433
7. G. 't Hooft: Nucl. Phys. B79 (1974) 276
8. A.S. Kronfeld, G. Schierholz, U.-J. Wiese: Nucl. Phys. B293 (1987) 461
9. A.M. Polyakov: JETP Lett. 20 (1974) 194
10. R. Jackiw, C. Rebbi: Phys. Rev. D13 (1976) 3398
11. C. Callias: Commun. Math. Phys. 62 (1978) 213
12. R.V. Gavai, H. Satz: Phys. Lett. 145B (1984) 248
13. I.M. Barbour et al.: In: The recursion method and its application, D.G. Pettifor, D.L. Weaire (eds.) Springer Series in Solid State Sciences 58. Berlin, Heidelberg, New York: Springer 1985
14. D.J. Gross, R.D. Pisarski, L.G. Yaffe: Rev. Mod. Phys. 53 (1981) 43
15. B. Berg: Phys. Lett. 104B (1981) 475
16. L.G. Yaffe, B. Svetitsky: Phys. Rev. D26 (1982) 963
17. A.S. Kronfeld, M.L. Laursen, G. Schierholz, U.-J. Wiese: Phys. Lett. 198B (1987) 516
18. N. Cabibbo, E. Marinari, Phys. Lett. 119B (1982) 387
19. G. Schierholz: In: Topological and geometrical methods in field theory. J. Hietarinta, J. Westerholm (eds.) Singapore: World Scientific 1986